Paper No :

MSAE2018-ARWM023

The Development Progress of Rubber Spectral Library for Different Rubber Clone

M. H. M. Hazir[1], A. K. Radhiah[2] and T. M. T. Muda[1]

[1]Div. of Extension and Development
Malaysian Rubber Board
Bangunan Getah Asli
148 Jalan Ampang, 50450
Kuala Lumpur, Malaysia

[2]Div. of Production Development
Malaysian Rubber Board
RRIM Research Station
40160 Sungai Buloh
Selangor, Malaysia

ABSTRACT

This paper presented progress development of fundamental study to understand rubber leaf spectral behavior based on different rubber clones. The different rubber clones will have specific shapes of the rubber leaf. Each clone also known has specialty to grow in specific soil, topography, disease resistance and environment conditions. This study indicate that different rubber leaves physical characteristics influence its spectral properties. Twenty samples reflectance value from each of four different rubber clones that covered the bandwidth of 400nm to 1000nm were collected. This data then can be transformed into valuable information to develop a spectral library that keeps previous, new and future rubber clone spectral signature information. The accuracy of the processing is much depending on the feature extraction techniques of hyperspectral data used. The result shows that near infra-red bandwidth and above had potential value to segregate rubber clones.

KEYWORDS

rubber clone, spectral library, reflectance

**Paper presented at the 2018 MSAE Conference, Serdang, Selangor D. E., Malaysia.
7 & 8 February 2018**

INTRODUCTION

A spectral reflectance property is based on the measurement of reflected or emitted radiation from different bodies. Objects having different surface features reflect or absorb the sun's radiation in different ways. Spectral reflectance, measured by the hyperspectral imaging equipment, is the amount of reflected light from a surface. Hyperspectral imaging is the process by which images are taken and numerical values (spectral radiance) assigned to each pixel, utilizing a range of wavelengths across the electromagnetic spectrum, including visible and infrared regions. Through the use of specialized software and statistical analysis, these pixels are sorted and characterized to distinguish between groups of pixels, or in the case of precision agriculture, plant characteristics and environmental conditions.

Earlier remote sensing technology, in particular multispectral imaging, collects data at a few widely-spaced wavelengths. The data from each wavelength band is assembled into a three-dimensional hyperspectral 'data cube' for processing and analysis. Each layer of the cube represents data at a specific wavelength. The concept of hyperspectral imaging originated at NASA's Jet Propulsion Laboratory in California with the development of the Airborne visible infrared imaging spectrometer (AVIRIS), able to cover the wavelength region from 400 to 2500 nm using more than 200 spectral channels, at nominal spectral resolution of 10 nm (Green, 1998).

The spectral characteristics of vegetation vary with wavelength. A compound in leaves called chlorophyll strongly absorbs radiation in the red and blue wavelengths but reflect a green wavelength. The internal structure of healthy leaves acts as a diffuse reflector of near-infrared wavelengths. Measuring and monitoring the infrared reflectance is one way that scientists determine how healthy particular vegetation may be. In reflecting-light spectroscopy the fundamental property that researchers want to obtain is spectral reflectance: the ratio of reflected energy to incident energy as a function of wavelength. Reflectance varies with wavelength for most materials because the energy at certain wavelengths is scattered or absorbed to different degrees. These reflectance variations are evident when we compare spectral reflectance curves (plots of reflectance versus wavelength) for different materials, as in the illustration in Figure 1.

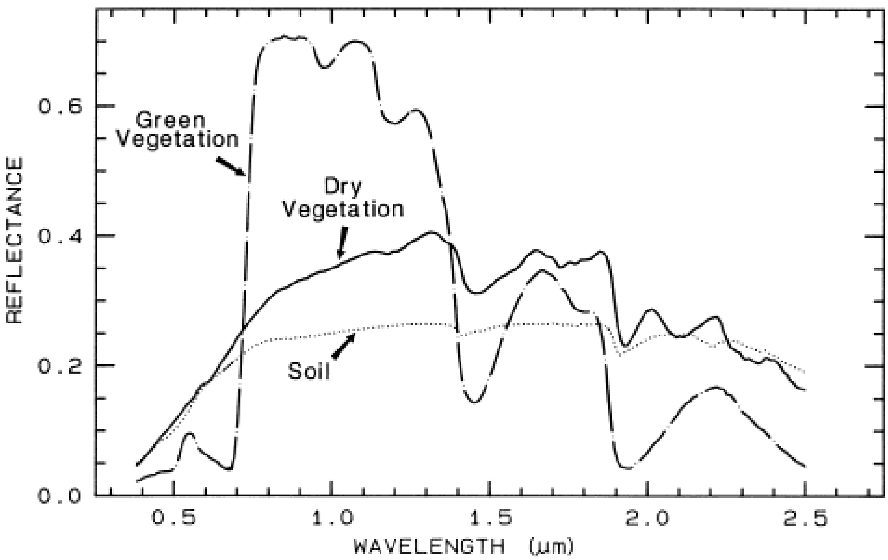

Figure 1. Plots of reflectance versus wavelength

Pronounced downward deflections of the spectral curves mark the wavelength ranges for which the material selectively absorbs the incident energy. These features are commonly called absorption bands (not to be confused with the separate image bands in a multispectral or hyperspectral image). The overall shape of a spectral curve and the position and strength of absorption bands in many cases can be used to identify and discriminate different materials. For example, vegetation has higher reflectance in the near infrared range and lower reflectance of red light than soils. Representative spectral reflectance curves for several common Earth surface materials over the visible light to reflected infrared spectral range. The spectral bands used in several multispectral satellite remote sensors are shown at the top for comparison.

Reflectance is a unit less quantity that ranges in value from 0 to 1.0, or it can be expressed as a percentage, as in Figure 2. When spectral measurements of a test material are made in the field or laboratory, values of incident energy are also required to calculate the materialist reflectance. These values are either measured directly or derived from measurements of light reflected (under the same illumination conditions as the test material) from a standard reference material with known spectral reflectance.

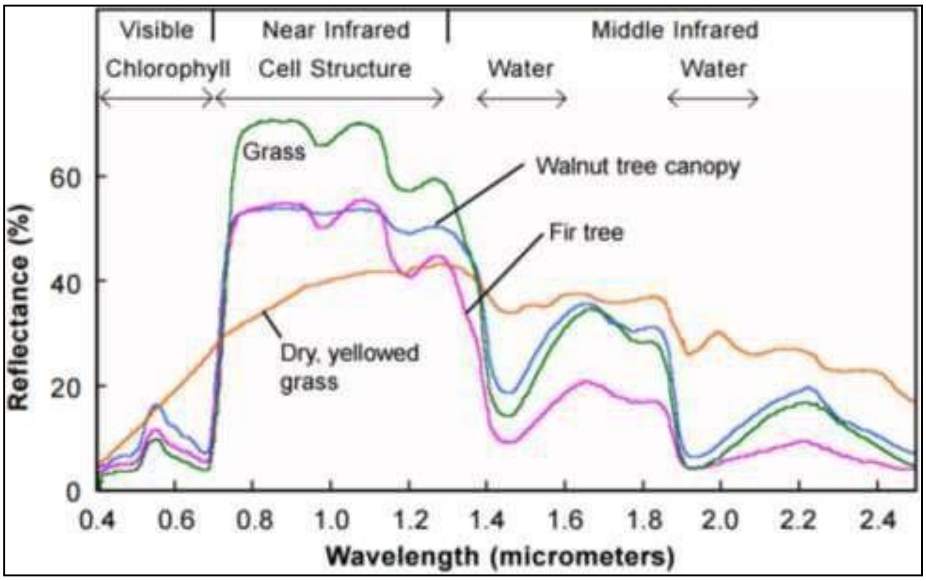

Figure 2. Reflectance value as a percentage

Figure 3 shows the study result of age based classification of Arecanut crops: a case study of Channagiri, Karnataka, India. It is observed from the analysis that crops of ages below 3, 3–7, 8–15 and above 15 years were showing distinct spectral behavior. It may be concluded that, not only age- based arecanut crop classification is possible, but also it is possible to develop age-based spectral library for plantation crops like arecanut (Bhojaraja et. al, 2015). Prasad and Gnanappazham (2014) study on discrimination of mangrove species of rhizophoraceae using laboratory spectral signatures. The objective was to determine potential wavelength locations in hyperspectral bands for the discrimination among eight mangrove species of the Rhizophoraceae family using their laboratory spectral reflectance data. Results have shown that red edge region is found to be the most consistent wavelength location to discriminate species. University of Wisconsin Environmental Spectroscopy Laboratory had published results of the spectral characterization of multiple corn varieties. The data were collected from 288 individuals belonging to 18 different corn varieties and examined to determine if varieties could be identified using spectra, and to determine how traits varied among varieties.

Leaf-level spectral data was collected in the summer of 2014 from corn plants located at the West Madison Agricultural Station in Madison, Wisconsin. 5 Measurements were taken from one leaf per plant. Collections occurred over the course of one day in the summer of 2014, using an ASD FieldSpec 3 spectrometer with leaf-clip contact probe. It can be viewed online through https://ecosis.org/#result/c0e238ea-5b23-452c-bc40- f0cfe2c6f032. Shwetank et. al, (2012) published the result on development of digital spectral library and supervised classification of rice crop varieties using hyperspectral image processing. Figure 4 shown the Spectral reflectance curves of various rice varieties in VNIR-SWIR bands. After pre-processing, the classification of rice crop at pixel scale across 155 calibrated spectral bands has shown promising result with 89.33% overall classification accuracy.

Meanwhile Pu (2008) study on an exploratory analysis of in situ hyperspectral data for broadleaf species recognition. The total of 394 reflectance spectra (between 350 and 2500 mm) from foliage, branches or canopy of 11 important urban forest broadleaf species were measured in the City of Tampa, Florida, U.S.

with a spectrometer. The 11 species include American Elm (Ulmus americana), Bluejack Oak (Q. incana), Crape Myrtle (Lagerstroemia indica), Laurel Oak (Q. laurifolia), Live Oak (Q. virginiana), Southern Magnolia (Magnolia grandiflora), Persimmon (Diospyros virginiana), Red Maple (Acer rubrum), Sand Live Oak (Q. geminata), American Sycamore (Platanus occidentalis), and Turkey Oak (Q. laevis). The preliminary results of identifying the 11 species with the in situ hyperspectral data imply that current remote-sensing techniques are still difficult but possible to identify similar species to such 11 broadleaf species with an acceptable accuracy.

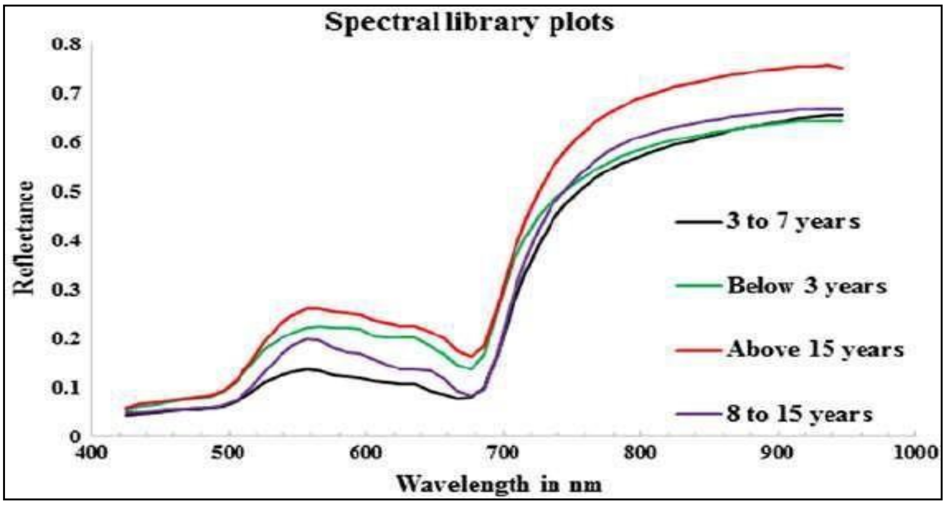

Figure 3. Spectral library for arecanut crops of different age groups

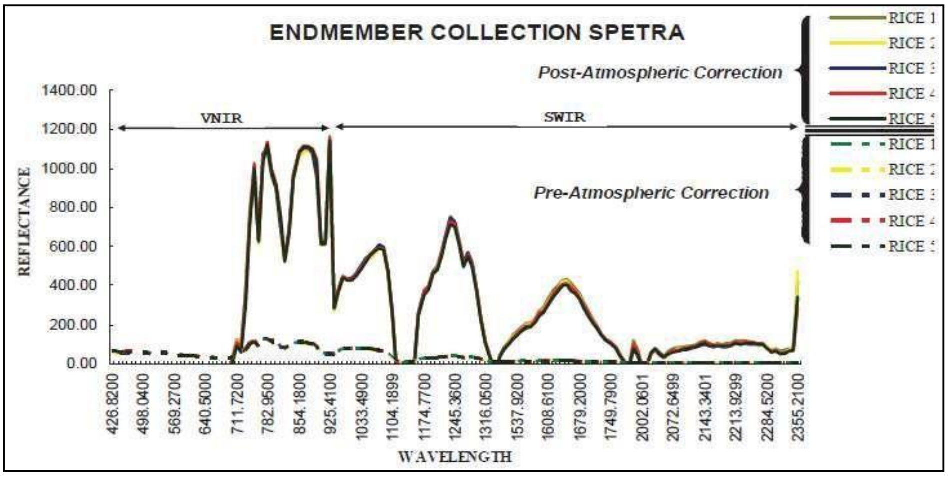

Figure 4. Spectral reflectance curves of various rice verities in VNIR-SWIR bands

The objective of this study is to collect spectral properties for rubber clones. This data then can be transformed into valuable information to develop a spectral library that keeps previous, new and future rubber clone spectral signature information. Later it could be used by researchers as a technical guideline and reference in any related rubber leaf, seed, bark and root spectral research or product development. It also broadens research opportunities in geospatial application and encourages more new findings from this field. The implementation of a spectral library is crucial and varies on applications.

2. MATERIALS AND METHODS

2.1. Study area

The selected study area was at Tapak Semaian RISDA Kesang Pajak (Nursery), Melaka, Malaysia (Figure 5). This nursery is owned by Rubber Industry Smallholders Development Authority (RISDA) and supplies most commercial rubber seedlings to smallholders. They also supply oil palm seedlings and others. MRB and RISDA always have strong collaboration and work closely as partners. The selection of seedling clones is based on the availability of commercial that have high demand. This study was conducted partly for Malaysian Rubber Board Scientific and Economic Advisory Council (SEAC) project where the objective is to develop a rubber clone spectral library.

Figure 5. Tapak Semaian RISDA Kesang Pajak (Nursery)

2.2. Hyperspectral Imager and Spectrometer

There were two types of equipment were used in this study. The first equipment was Hyperspectral Imager (Figure 6). The OCI™-F (OCI is a phonetic spelling of "All Seeing Eye") camera is a miniaturized push-broom hyperspectral camera covering the full VNIR (400-1000 nm) wavelength range, with SuperSpeed USB 3.0 interface. It features ultra-compactness (15 cm x 5 cm x 9 cm) and light weight (~550 g) with super-fast data transfer rates (up to 50 fps). As an innovative "true push-broom" imager: one can simply use a hand to move the imager or sample to finish the scan. Not depending on a constant scanning speed has enabled OCI-F versatility on vast platforms such as UAVs with perfect hyperspectral imaging stitching. Compactness, fast imaging, simple operation, and intuitive software make the OCI-F very straightforward for applications such as precision agriculture, remote sensing, forensics, and airborne applications. The second equipment was spectrometer (Figure 7). The USB2000+UV-VIS is a miniature spectrometer pre-configured for general UV-VIS measurements. Covering a wide wavelength range, from 200 to 850 nm, this high-performance spectrometer fits into the palm of human hand giving the measurements new flexibility. Using the modular approach, it can be customized measurement with wide array of sampling accessories and light sources.

Figure 6. Hyperspectral Imager

Figure 7. Spectrometer

2.3. Rubber seedling

30 samples from each 4 rubber clones were selected for this study (Figure 7). Two clones were from Group 1 namely RRIM 2002 and PB350. The remaining two were from Group 2 namely RRIM 2025 and 3001. All these clones are commercial types that have high demand on the market. The seedlings must meet on certain criteria to make sure this study gets viable results. The selected seedlings need to be in the two leaf stage or 2 whorls and healthy. The leaves are required to be in good condition and clean.

Figure 8. Rubber Seedling Clones

2.1. Data collection, pre-processing and analysis

The data collection process was completed in an indoor setting, in order to control light resources and avoid sunlight. Even though it can be done in an outdoor environment, the decision was made to make sure this method can be repeated elsewhere. The selected leaves were cut and put on black background before the measurement started. Figure 8 shows the Hyperspectral data collection process begins with setup the equipment. Then, all leaves were scanned using Hyperspectral. After that, the raw data were transferred to the computer storage. BaySpec's SpecGrabber were used for camera control and data acquisition. The raw hyperspectral data then were processed into readable data using CubeCreator software. Meanwhile, for the spectrometer, the raw data are in .txt format and can be converted to excel file for further analysis. The upper part of the leaf is measured because of mesophyll cells are concentrated here. Mesophyll contain chloroplasts for photosynthetic reactions. Each clone reacts uniquely based on the unique structure of the leaf. It was repeated to all samples. The data were then analyzed using ENVI software to perform spectral library properties.

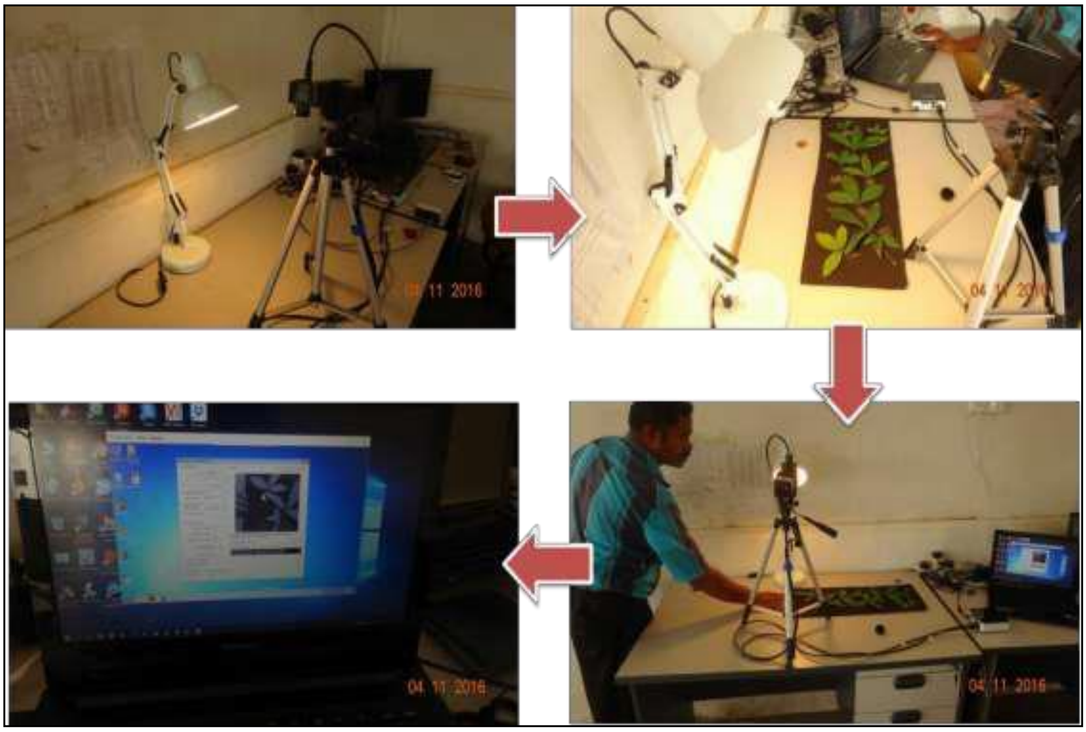
Figure 9. Data collection using hyperspectral imager


Figure 10. Data collection using spectrometer

2.2. Leaf lamina anatomical characteristics

The lamina characteristics of each rubber clone were analyses using microscope. The focus area to be look into detail was lamina because of the target area during collecting data using spectrometer and hyperspectral was there.

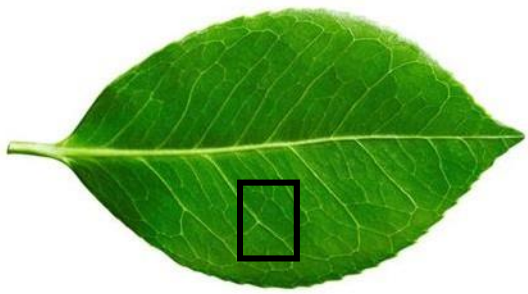

Figure 11. Lamina section

3. RESULTS AND DISCUSSIONS

The results show (Figure 12 and Figure 13) there are potentials using hyperspectral and a spectrometer to distinguish rubber clones. Each clone gave unique spectral library information. Both hyperspectral and spectrometer analyses give consistent result as the infra-red bandwidths and above give distinctive values among rubber clones. Figure 14 indicate that each clone had specific characteristics of anatomy. Further study will clarify in detail on this particular subject. It's the best reason so far why each clone gives different spectral properties result.

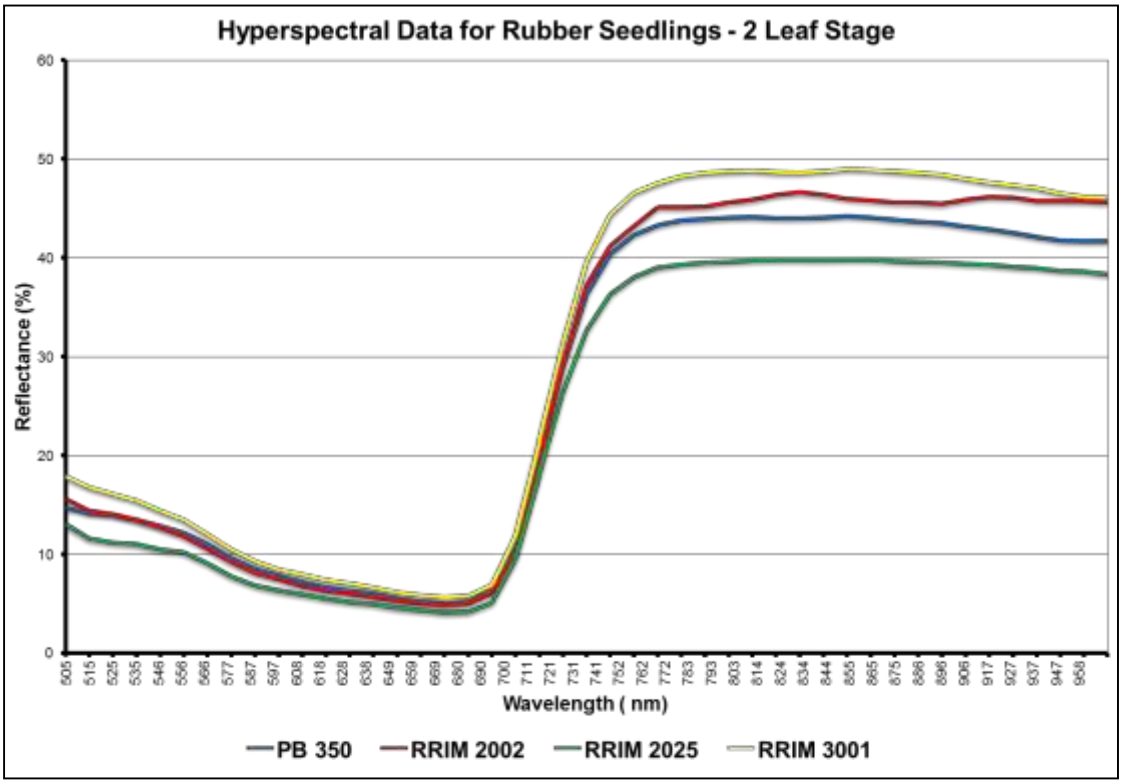

Figure 12. Hyperspectral result

ISBN 978-967-16145

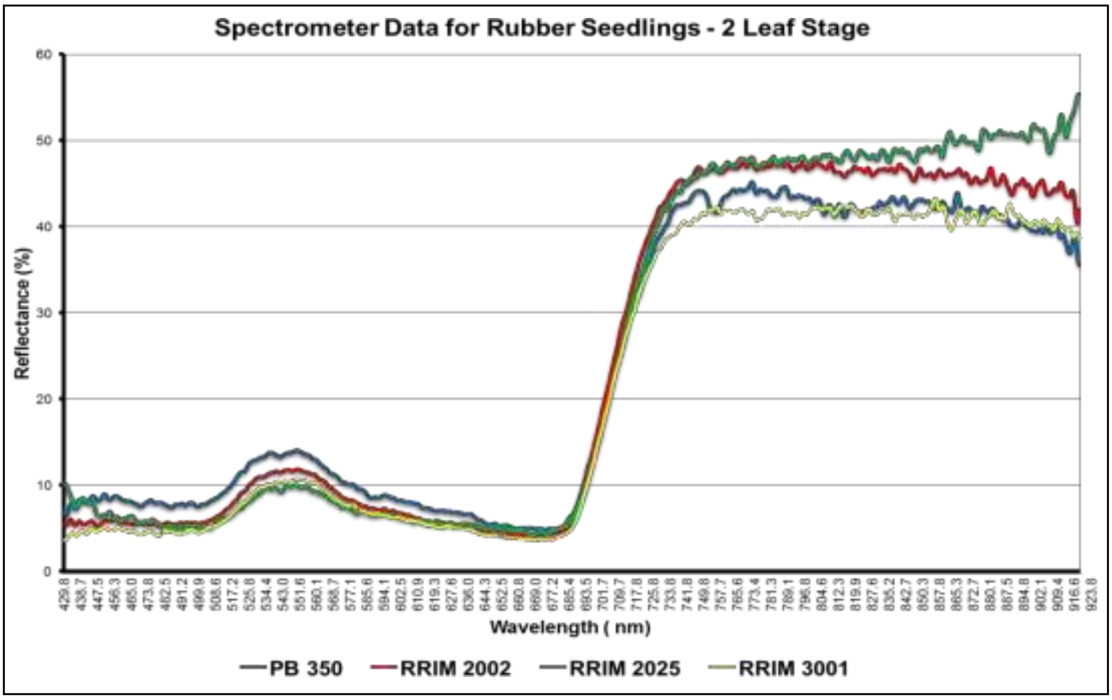

Figure 13. Spectrometer result

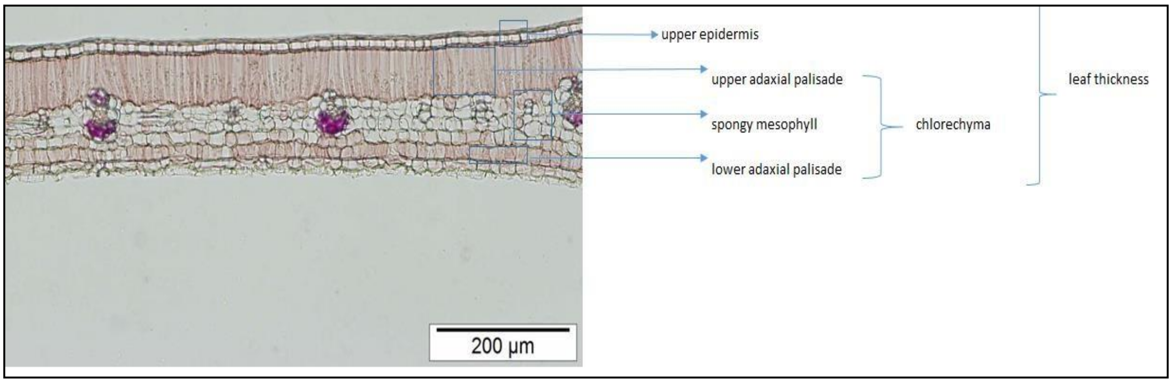

Figure 14. Lamina anatomical section

4. CONCLUSIONS

Hyperspectral and spectrometer information of rubber leaf in nursery stage was successfully collected for 4 clones. Rubber leaf hyperspectral/spectrometer properties for different clones were compared and showed promising results. The unique characteristics of individual rubber clones by segregation from others based on rubber leaf hyperspectral/spectrometer information still open for further analysis and findings.

ACKNOWLEDGEMENT

This study was partly conducted under Extension and Development Division and supported fully by the Malaysian Rubber Board. Appreciation goes to Mr. Zarawi Bin Ab. Ghani, Nurmi Rohayu Abdul Hamid, Irwan Amin Bin Suggun, Zakaria Bin Muhammad Shah, Zuleffendy Bin Mohd Yusop, Kumar A/L Veliayudam – Ornet Sdn. Bhd., Malaysian Rubber Board, RISDA Semaian Sdn. Bhd. Special thanks go to Extension and Development Department staff and whoever contributed to this study.

References

1. Camps-Valls G., Gómez-Chova L., J. Muñoz-Marí, J. L. Rojo-Álvarez, and M. Martínez-Ramón, "Kernel-based framework for multitemporal and multisource remote sensing data classification and change detection," IEEE Transactions on Geoscience and Remote Sensing, vol. 46, no. 6, pp. 1822–1835, 2008.View at Publisher · View at Google Scholar · View at Scopus
2. Camps-Valls G., Gomez-Chova L., Muñoz-Marí J., Vila-Francés J., and J. Calpe-Maravilla, "Composite kernels for hyperspectral image classification," IEEE Geoscience and Remote Sensing Letters, vol. 3, no. 1, pp. 93–97, 2006. View at Publisher · View at Google Scholar · View at Scopus
3. Clark, R. N., and Swayze, G. A., 1995, Mapping minerals, amorphous materials, environmental materials, vegetation, water, ice, and snow, and other materials: The USGS Tricorder Algorithm: in Summaries of the Fifth Annual JPL Airborne Earth Science Workshop, JPL Publication 95-1, p. 39-40.
4. G. Camps-Valls and L. Bruzzone, "Kernel-based methods for hyperspectral image classification," IEEE Transactions on Geoscience and Remote Sensing, vol. 43, no. 6, pp. 1351–1362, 2005. View at Publisher ·View at Google Scholar · View at Scopus
5. Goetz, A. F. H., 1993, The spectral image processing system (SIPS) - Interactive visualization and analysis of imaging spectrometer data: Remote Sensing of Environment, v. 44, p. 145-163.
6. Gonçalves, P. D. S., Scaloppi Júnior, E. J., Martins, M. A., Moreno, R. M. B., Branco, R. B. F., & Gonçalves, E. C. P. (2011). Assessment of growth and yield performance of rubber tree clones of the IAC 500 series. Pesquisa Agropecuária Brasileira, 46(12), 1643- 1649.
7. Green R. O., Imaging spectroscopy and the airborne visible-infrared imaging spectrometer (AVIRIS), Remote Sensing of Environment, 65, 227–248, 1998.
8. Jusoff, Kamaruzaman; Ismail, Mohd Hasmadi; Ali, Nurul Hidayah Mohd. Journal of Environmental Science and Engineering3.1 (Jan 2009): 37
9. Kruse F. A., LefkofA. B. f, Boardman J. W. et al., "The spectral image processing system (SIPS)-interactive visualization and analysis of imaging spectrometer data," Remote Sensing of Environment, vol. 44, no. 2-3, pp. 145–163, 1993. View at Publisher · View at Google Scholar · View at Scopus
10. Kruse, F. A., Lefkoff, A. B., Boardman, J. W., Heidebrecht, K. B., Shapiro, A. T., Barloon, J. P., and
11. Lau, Alvin Meng Shin and Hashim, Mazlan (2007) The design and building of spectral library of tropical rain forest in Malaysia. In: The 28th Asian Conference on Remote Sensing 2007, 12-16 November 2007, PWTC, Kuala Lumpur, Malaysia.
12. Lau, C. H., & Wong, C. B. (1993). Correction of leaf nutrient values for assessment of Hevea nutrition. In Plant Nutrition—from Genetic Engineering to Field Practice (pp. 281- 283). Springer Netherlands.
13. Lau, C. H., Wong, C. B., & Chin, H. C. (1990). A modified procedure for foliar sampling of Hevea brasiliensis. Journal of Natural Rubber Research, 5(3), 224-230.
14. Lokmal, N., Zaki, A. M., Fazwa, M. F., Suhaimi, W. C., Azmy, Y., Zakaria, I., ... & Wan-Akil, T. A. (2008). Growth of several rubber clones for timber production. Journal of Tropical Forest Science, 175-180.
15. Maulik U. and Bandyopadhyay S., "Fuzzy partitioning using a real-coded variable-length genetic algorithm for pixel classification," IEEE Transactions on Geoscience and Remote Sensing, vol. 41, no. 5, pp. 1075–1081, 2003. View at Publisher · View at Google Scholar · View at Scopus
16. Melgani F. and Bruzzone L., "Classification of hyperspectral remote sensing images with support vector machines," IEEE Transactions on Geoscience and Remote Sensing, vol. 42, no. 8, pp. 1778–1790, 2004.View at Publisher · View at Google Scholar · View at Scopus
17. Miao, Z., & Shi, W. (2015). A New Methodology for Spectral-Spatial Classification of Hyperspectral Images. Journal of Sensors, 2016.
18. Mohd Nasarudin, Nurul Ezaty and Mohd Shafri, Helmi Zulhaidi (2011) Development and utilization of urban spectral library for remote sensing of urban environment. Journal of Urban and Environmental Engineering, 5 (1). pp. 44-56. ISSN 1982-3932
19. Pal M. and Mather P. M., "Support vector machines for classification in remote sensing," International Journal of Remote Sensing, vol. 26, no. 5, pp. 1007–1011, 2005. View at Publisher · View at Google Scholar· View at Scopus
20. Plaza, A., Benediktsson, J. A., Boardman, J. W., Brazile, J., Bruzzone, L., Camps-Valls, G., ... & Marconcini, M. (2009). Recent advances in techniques for hyperspectral image processing. Remote sensing of environment, 113, S110-S122.
21. Plaza, A., Plaza, J., Paz, A., & Sanchez, S. (2011). Parallel hyperspectral image and signal processing [applications corner]. IEEE Signal Processing Magazine, 28(3), 119-126.

22. Shafri H. Z. M., Suhaili A., and Mansor S., “The performance of maximum likelihood, spectral angle mapper, neural network and decision tree classifiers in hyperspectral image analysis,” Journal of Computer Science, vol. 3, no. 6, pp. 419– 423, 2007. View at Publisher · View at Google Scholar
23. Tso B. C. K. and Mather P. M., “Classification of multisource remote sensing imagery using a genetic algorithm and Markov random fields,” IEEE Transactions on Geoscience and Remote Sensing, vol. 37, no. 3 I, pp. 1255–1260, 1999. View at Publisher · View at Google Scholar · View at Scopus.